Published in IET Microwaves, Antennas & Propagation
Received on 18th June 2014
Revised on 3rd September 2014
Accepted on 8th September 2014
doi: 10.1049/iet-map.2014.0408

ISSN 1751-8725

A 60 GHz simple-to-fabricate single-layer planar Fabry–Pérot cavity antenna

Alister Hosseini, Franco De Flaviis, Filippo Capolino

Henry Samueli School of Engineering, Electrical Engineering and Computer Science Department, University of California, Irvine, CA 92697, USA
E-mail: sahossei@uci.edu

Abstract: A planar single-layer single-feed Fabry–Pérot cavity antenna is designed and fabricated to operate at 60 GHz. The simplicity and planarity of this design is achieved by using only a laminated and commercially available dielectric slab, forming the cavity of the antenna, and by exciting the antenna through a planar feed, that is, a coplanar-waveguide-fed slot-dipole, printed directly on the ground plane of the cavity. The backward radiation because of a feeding-slot on the ground plane of the cavity is also investigated and a new closed form formula is presented. The radiation performance of the fabricated antenna is measured using an automated measurement setup built to characterise high-gain millimetre-wave antennas being probed on the opposite side of the main radiation beam.

1 Introduction

Highly efficient high-gain antennas are desired for 60 GHz wireless systems to compensate the path loss associated with the wireless link. Besides array antennas as in [1], Fabry–Pérot cavity (FPC) antennas are also known for being able to produce highly efficient directive radiation [2, 3]. Only a handful of millimetre-wave (MMW) FPC antennas have been designed, fabricated and measured, as for example those reported in [4–7]. In this paper, following the introductory works in [8, 9], a 60 GHz single-layer FPC antenna excited by an integrated planar feed (i.e. a coplanar-waveguide-fed slot-dipole) will be investigated. The main differences between the proposed antenna and the previous works can be explained as follows.

First, the previously proposed MMW FPC antennas were made of air-filled cavities (i.e. cavities filled mainly with air) covered by a thick partially reflective surface (PRS) (i.e. the thickness of PRS is comparable with the maximum wavelength in the operational frequency band, for example, stack of multi-layer dielectric slabs as in [4, 6], a quasi-planar dual-layer PRS made of a non-uniform curved metallic grid on top of a uniform one, as in [5], or a thick metallic frequency selective surface (FSS) as in [7]). However, in this paper, the cavity is only made of a single dielectric slab. Using a standard substrate (from Rogers Corporation) as the cavity, gives us the opportunity of printing the FSS and ground plane on each side of the dielectric substrate using, for example, a standard low-cost lithography and etching process. Being able to fabricate a single-layer MMW FPC antenna with a thin FSS, as opposed to what has been done in [4–7], simplifies the transmission line model of the antenna providing a straightforward design procedure for this type of cavity, as shown in [8, 9]. Second, without adding any extra layer to the antenna structure, a planar integrated feeding line is proposed directly on the ground plane of the cavity. This feeding line provides the opportunity of integrating the antenna to other millimetre-wave components on the same substrate proposing a promising solution from an MMW technological standpoint.

In this paper, following the introductory discussion in [8, 9], novel investigations are carried out on the radiation performance of such cavities designed at MMWs. For FPCs fed by an integrated planar feeding-slot (e.g. a coplanar-waveguide-fed slot-dipole) on their ground plane, the backward radiation is investigated here for the first time resulting in a simple and novel analytical formula which can be used to estimate forward-to-backward (F/B) radiation ratio of such FPC antennas. Moreover, looking at F/B radiation ratio and the gain bandwidth of the proposed design, the advantages and shortcomings of this type of FPC antenna are briefly discussed. Finally, besides introducing our dedicated measurement system at MMWs along discussing its main advantages over previously published systems, a complete set of measurement results are shown and compared with full-wave simulation results.

2 Theoretical design and radiation performance

The general structure of the proposed antenna is shown in Fig. 1. An RT/duroid 5880 substrate with nominal relative permittivity of $\varepsilon_r = 2.3$, dielectric loss tangent of tan $\delta = 0.0009$, and nominal thickness h of 1.575 mm, is selected for this design. The metallisation on both sides of the substrate uses 7 μm copper layer. Please see [8, 9] for more

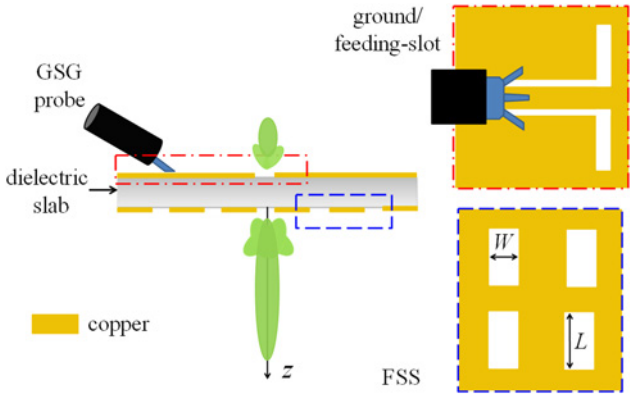

Fig. 1 *Layered view of the proposed FPC antenna made of a single-layer dielectric-slab cavity and fed by a ground–signal–ground probe from the top (i.e. from the ground plane)*

It can be seen that the cavity mainly radiates downwards, through the FSS, while a small backward radiation is expected through the feeding-slot on its ground plane

information on theoretical design steps of this antenna. As discussed in [2, 3, 8, 9], a thin metallic FSS can be modelled as shunt susceptance in the transmission line (TL) model of the antenna. The dimensions of the periodic slots in a squared unit-cell and the normalised (to $Y_0 = 377\ \Omega$) susceptance representing the FSS in a transmission line model (i.e. $\hat{b}$) against frequency is shown in Fig. 2*a*. Using the derived FSS model, based on formulas in [10] as also discussed in [9], the analytical broadside (i.e. along z as shown in Fig. 1) radiation gain of the designed antenna is estimated as shown in Fig. 2*b*. It can be seen that the maximum theoretical gain of the designed antenna is 16.7 dB at 59.5 GHz.

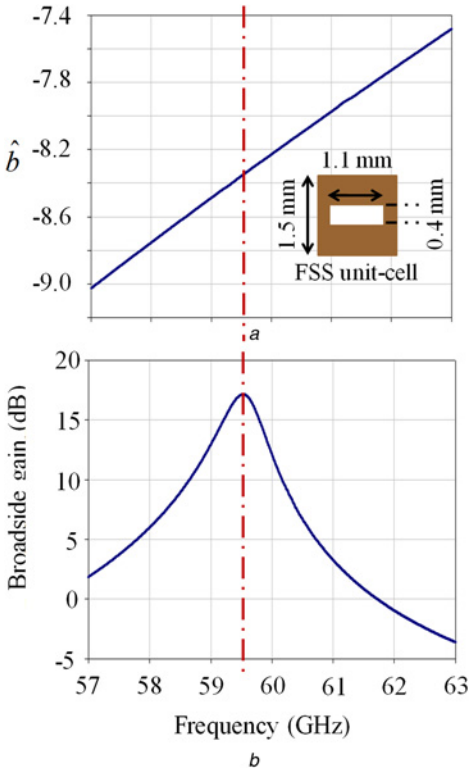

Fig. 2 *Theoretical study of the proposed antenna*

a Normalised susceptance modelling the designed FSS against frequency
b Theoretical broadside radiation gain against frequency

Considering the feeding method of the proposed antenna, the back-radiation or F/B radiation ratio, becomes an important issue to be addressed here. The TL model of the FPC antenna, shown in [9], can be used to derive a simple formula to estimate (F/B). Based on TL model of the antenna and using the related formulas discussed in [11], the feed (i.e. a magnetic current) is modelled as voltage source v_s providing power for both the FPC and the half space below the ground plane, as shown in Fig. 3. The time-averaged power density radiated from the feeding-slot at broadside, above and below the antennas (i.e. the power delivered by the voltage source for the up and downward circuits shown in Fig. 3) can be expressed as $P_{\text{up}} = \frac{1}{2}|v_s|^2 \text{Re}\left(Y_{\text{up}}^*\right)$ and $P_{\text{down}} = \frac{1}{2}|v_s|^2 \text{Re}(Y_{\text{down}}^*)$, respectively, where Y_{up} is he equivalent admittance derived from the TL model, looking in the $+z$-direction inside the cavity as shown in Fig. 3, and $Y_{\text{down}} = Y_0$ is the free space wave admittance. The (F/B) ratio is evaluated looking at the far-field angles of 0 and 180°, therefore the TL equivalent admittances should be evaluated for these directions, that is, normal to the antenna plane. This results in (F/B) calculated as

$$(\text{F/B}) = \frac{P_{\text{up}}}{P_{\text{down}}} = \frac{\text{Re}\left(Y_{\text{up}}^*\right)}{\text{Re}\left(Y_{\text{down}}^*\right)} = \varepsilon_{\text{r}} \frac{\cot^2(kh) + 1}{\bar{B}_{\text{tot}}^2 + 1} \tag{1}$$

where $\bar{B}_{\text{tot}} = \sqrt{\varepsilon_{\text{r}}}\cot(kh) - \hat{b}$ vanishes at the resonance frequency of the cavity (please see [9]) and $k = 2\pi f\sqrt{\mu_0\varepsilon_0\varepsilon_{\text{r}}}$ is the wavenumber in the dielectric material inside the FPC.

Fig. 4*a* shows (F/B) of single-layer FPCs, resonating at 59.5 GHz, filled with a fixed material (i.e. $\varepsilon_{\text{r}} = 2.3$) and formed by using various FSS layers with different reflectivities (i.e. achieved by changing the lengths of the periodic slots (i.e. L) while keeping their width $W = 0.4$ mm where $L = 1.1$, 1.2, 1.3 and 1.4 mm corresponds to cavities with maximum gain of 16.7, 13, 10.3 and 7 dB, respectively). It can be seen, by decreasing the maximum gain of the FPC antenna (i.e. lower reflectivity of the FSS), (F/B) drops significantly. Similarly, (F/B) increases significantly by increasing the relative permittivity of the FPC dielectric, as shown in Fig. 4*b*, for FPCs designed to resonate at 59.5 GHz with fixed maximum gain of 17 dB. These designs have been achieved by changing the unit-cell

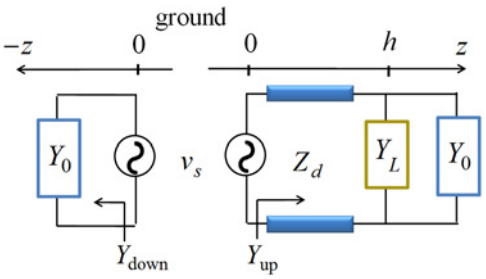

Fig. 3 *Circuit model for forward and backward radiation of the antenna fed by a slot on the ground plane, modelled as a voltage generator*

doi: 10.1049/iet-map.2014.0408

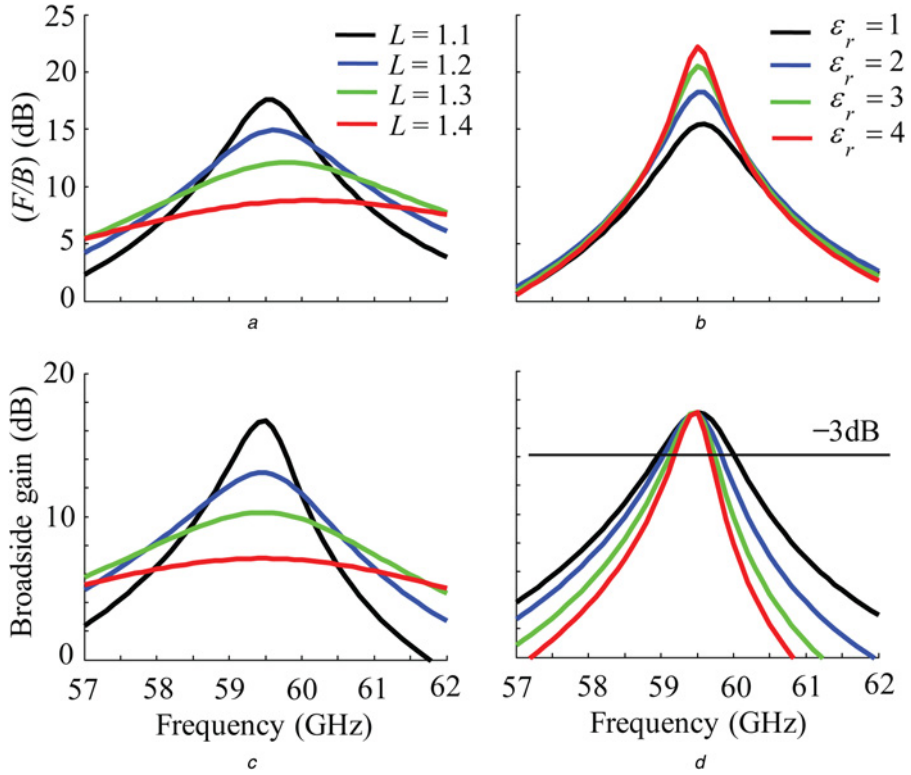

Fig. 4 *Theoretical broadside gain and (F/B) of single-layer FPC*

a (F/B) of FPCs resonating at 59.5 GHz for various FSS design (achieved by varying the length of the periodic slots, i.e. *L*, in millimetres). Note, in these simulations, all the cavities are formed on substrate with a relative permittivity of $\varepsilon_r = 2.3$

b (F/B) of FPC antennas designed with various permittivities of the material filling the cavity. In these antennas, the dimensions of the periodic slots along with the unit-cell sizes are changed to achieve a fixed maximum gain of 17 dB at 59.5 GHz for all cases.

c The broadside radiation gain of cavities designed in (a) varying frequency

d The broadside radiation gain of cavities designed in (b) varying frequency

(still squared and determined by the side dimension of *U*) and the slot dimensions for each permittivity value (i.e. $(U, L, W) = (2.25, 1.5, 0.6$ mm) for $\varepsilon_r = 1$, $(U, L, W) = (1.5, 1.085, 0.4$ mm) for $\varepsilon_r = 2$, $(U, L, W) = (1.35, 0.93, 0.35$ mm) for $\varepsilon_r = 3$ and $(U, L, W) = (1.15, 0.795, 0.3$ mm) for $\varepsilon_r = 4$).

The analytical broadside radiation gain of the designed cavities in Figs. 4*a* and *b* are calculated following the steps in [10] and are shown in Figs. 4*c* and *d*, respectively. From Fig. 4*d*, it can be observed that the broadside gain bandwidth of the antenna decreases by increasing the relative permittivity of the dielectric slab (assuming a constant maximum gain).

Looking at the plots shown in Fig. 4, the advantages and disadvantages of the proposed design can be summarised as below. By replacing an air-field cavity with a dielectric slab, besides having a thinner antenna, (F/B) increases significantly, while this results in smaller gain bandwidth for the antenna. Although the backward radiation of this antenna is negligible, to further decrease its level, another layer of a laminate with one side of copper-coating can be placed behind the slot-dipole; however, its presence should be included in the input matching procedure of this antenna.

3 Measurement against simulated results

A detailed figure of the fabricated antenna and its feeding line, along with a table of dimensions, can be found in [9]. However, for sake of completeness, general snapshots of the top and bottom views of the fabricated antenna are shown in Fig. 5. The antenna is fabricated using standard low-cost printed circuit board technology relying on single dielectric layer two-side metallisation without interconnecting vias. The entire fabrication process including lithography, double-sided mask alignment and

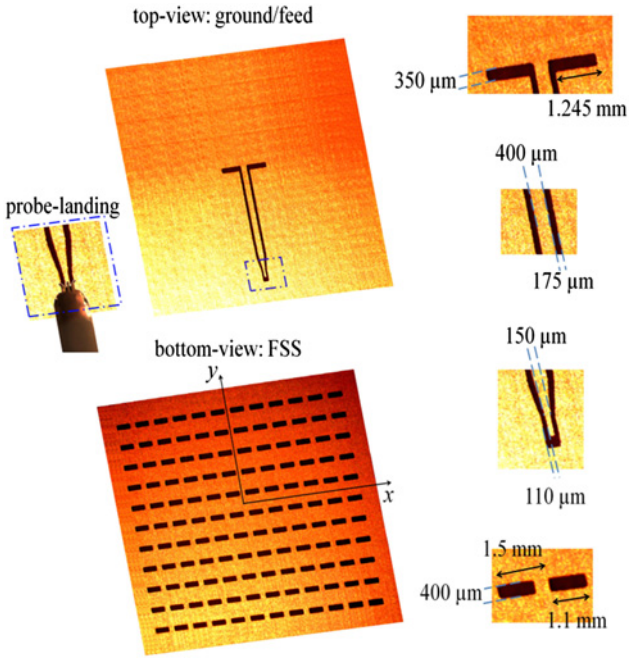

Fig. 5 *Microphotographs of the top (i.e. feed/ground) and bottom (i.e. FSS) views of the fabricated antenna. The top face is probed, the bottom side radiates as shown in Fig. 1*

wet-etching process of copper, has been carried out manually in our dark-room/wet-lab at the University of California, Irvine. To fabricate the antenna, the FSS (ideally extended infinitely in its plane, here *xy*-plane as shown in Fig. 5) must be truncated transversely. The number of the FSS elements (12×12) are selected aiming for negligible field strength at the edges of the transversely truncated cavity; the strength of the leaky-wave field at various distances from the centre of the antenna (i.e. where the feed is located) can be found using formulas discussed in [10].

The radiation performance of the antenna is measured with our dedicated automated system, as shown in Fig. 6, built to measure the radiation performance of high-gain MMW antennas being probed from the top, that is, on the opposite side of the main radiation hemisphere of the antenna.

The system consists of a probe positioner mounted on a large plexiglas plate, where a square hole in the centre of the plate is used to support the antenna leaving free its radiating side. Probing is done on the back side (with respect to the radiation), therefore the antenna is free to radiate downwards during probing (as also shown in Fig. 1). The system is mounted on an optically isolated table for easy probing, equipped with a digital microscope. A computer-controlled rotating arm with a V-band receiver (terminated with an open-ended waveguide) moves around the antenna to collect its radiation. Antenna, probe and receiver antenna can be rotated by 90° individually, to allow collecting four radiation patterns at each frequency (*E*-plane, *H*-plane, Co-pol and Cross-pol). A reference horn antenna (with the maximum gain of $G_H = 21$ dB) is used to calibrate the system and extract the absolute gain information of our antenna (by replacing the antenna under test (AUT) while keeping the same distance to the receiving antenna placed on the rotating arm). We then measure the output/input power ratios for the AUT and REF, of the two systems with the fabricated antenna and the reference horn antenna in place, respectively. After considering all the insertion losses in the waveguide-to-horn transition (L_T) and in the probe-tip (L_P), the radiation gain of the fabricated antenna is estimated as

$$G = G_H + \left[(\mathrm{AUT} + L_P) - (\mathrm{REF} + L_T)\right] \qquad (2)$$

where AUT and REF (both in dBm) are the received power by the power-meter when the transmitting antenna is the antenna under test and the horn antenna, respectively

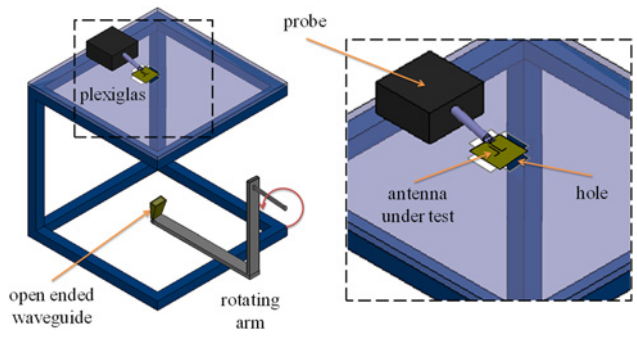

Fig. 6 *Measurement setup built to measure both reflection coefficient and radiation patterns of a fabricated antenna at MMW frequencies*

Probing of the AUT is on the top side. The antenna is mounted on a plexiglas plane with a hole for letting the antenna radiation be directed on the bottom side where a receiving open-ended waveguide is mounted on a rotating arm

Considering previous systems, for example, one discussed in [12], our measurement system shows some advantages which can be highlighted as below:

- The system is fully automated resulting in very accurate measured values in accurate desired positions and angles. Furthermore, besides significantly reducing the human error factor, the accuracy of the measurement plots can be improved by increasing the measurement samples.
- The antenna is probed from the top, on the opposite side of the main radiation occurring in the bottom hemisphere; therefore, the bulky structure of the probe does not distort the measured patterns.
- The AUT is placed more than 150 wavelengths away from the measuring antenna (to assure both antennas are in the far-field region of each other).
- Since the antennas are far-apart from each other, the path loss is significant (i.e. more than 65 dB) requiring a system with very low noise-floor (i.e. high dynamic range) to make sure we can capture all the details in the co-pol and cross-pol patterns. It is a known fact that losses of cables and connectors at very high-frequencies (e.g. at MMWs) are significantly larger than those of lower frequencies (e.g. microwaves). To minimise the use of high-frequency cables and connectors, the high-frequency circuitry of our measurement setup is minimised. This has been achieved by down-/up-converting blocks as will be explained shortly. The power is produced at a medium

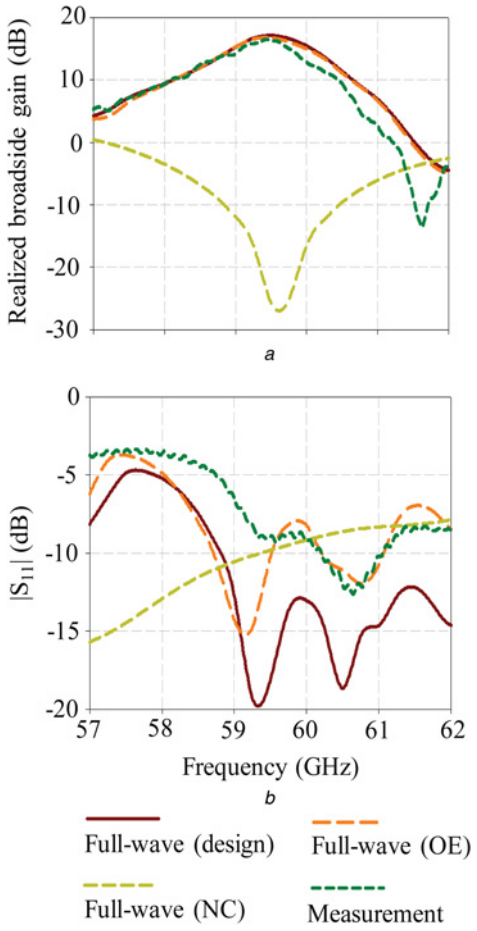

Fig. 7 *Measurement against simulated results*

a Broadside realised gain of the antenna
b Magnitude of input reflection coefficient of the antenna (S_{11} in a 50 Ω reference system). Comparison among the simulated designed antenna, simulated OE antenna, simulated antenna with no cover/FSS (NC), and measurement of the fabricated antenna

doi: 10.1049/iet-map.2014.0408

frequency (here, in Ku band), then by passing through an up-converting block excites the transmitting antenna (here, the AUT). On the other side, the radiated power is received by the receiving antenna (here, the open-ended waveguide) which will be down-converted to the medium frequency and measured by a highly sensitive power-meter.

Fig. 7*a* shows the realised broadside radiation gain of the fabricated antenna compared with its full-wave simulated values against frequency. Full-wave simulations are carried out by using a finite-element-based simulation software (here, high-frequency structure simulator (HFSS) by ANSYS Corporation). The maximum gain of the antenna, at 59.45 GHz (i.e. very close to the resonance frequency of the cavity at 59.5 GHz), was measured to be ∼16.5 dB, whereas the analytical (based on the TL model) and the simulated (full-wave) ones are about 16.7 and 17.15 dB at 59.5 GHz, respectively. The simulated and measured 3 dB gain bandwidth values (i.e. the frequency range within which the broadside radiation gain of the antenna remains above −3 dB level of its maximum value) of the antenna are equal to 1.4 and 1.2 GHz, respectively. Fig. 7*b* shows the measured reflection coefficient compared with the full-wave result of the designed antenna (design). It can be seen that the reflection coefficient of this antenna has two resonances; one at the peak-gain frequency of 59.5 GHz and one at 60.5 GHz. Although the measured plot has a very similar frequency-response to the simulated one (using full-wave simulations), there are some differences in the measured levels of reflection coefficient of the antenna which can be explained by sensitivity simulations as follows.

To assess the sensitivity of the design to the accuracy of the small geometrical features of the feed, we compared simulated gain and input reflection coefficient values of the design with those of an over-etched (OE) feed scenario. As previously mentioned, the fabrication of the antenna is carried out manually by illuminating the surfaces of the substrate being covered by patterned photo-resist material and then wet-etching the copper layers on both sides of substrate. The minimum gap and trace width of this design (in its feeding structure, as shown in Fig. 5) are equal to 110 and 150 μm, respectively. For the OE antenna feed, it is assumed that the feeding structure of the antenna is OE by 25 μm, that is, the width of metallic traces is decreased by 25 μm while the width of gaps are increased by 25 μm. For large features of the design as in the periodic slots forming the FSS and the slot-dipole feed, 25 μm is only 6 and 7% of their minimum dimensions (here, width of the periodic slots and the slot-dipole feed), respectively, while for the feeding structure, this value represents about 23% change in its minimum design parameter (i.e. gap width of 110 μm) which is not negligible anymore. Moreover, the over-etching process does not change the thickness of the slab, therefore the height of the cavity remains unchanged. In Fig. 7*b*, we show the simulated results for the reflection coefficient also for the OE antenna. It can be seen that the simulated results for the OE antenna has a closer response to measured reflection coefficient of the fabricated antenna explain that some over etching may have occurred in the fabrication steps.

Moreover, looking at Fig. 7*a*, the antenna with the nominal design values but without the FSS layer (i.e. with no cover (NC)) has a significantly lower broadside gain comparing

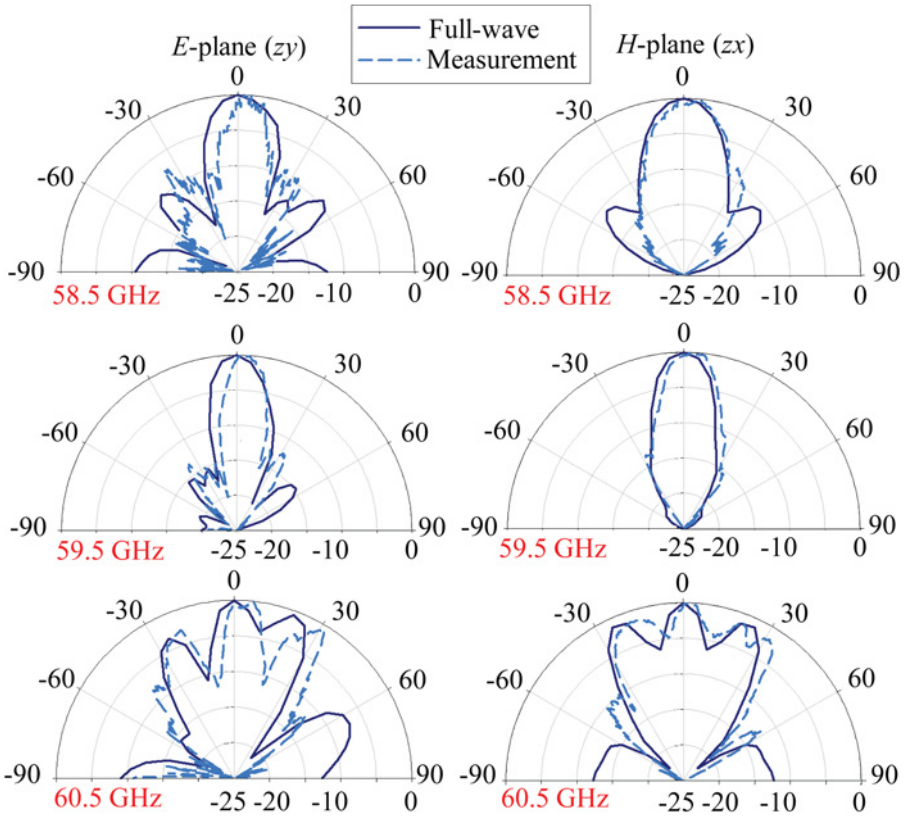

Fig. 8 *Co-pol radiation patterns of the fabricated antenna in both E and H planes, a comparison between the simulation and measurement results*

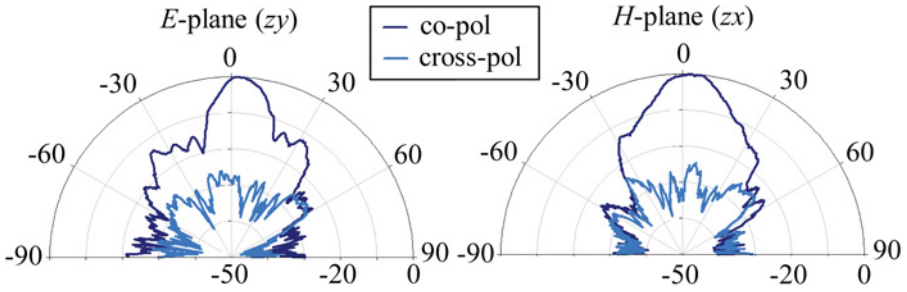

Fig. 9 *Comparison between measured co-pol and cross-pol patterns of the antenna, measured at 59.5 GHz, in both E and H planes*

with the proposed design. This shows that the broadside gain of the antenna is mainly a function of the reflectivity of the FSS and not the gain of the feeding antenna whose role is only to excite the leaky-waves inside the cavity, that are responsible for the directive pattern at broadside [2, 3]. Looking at the reflection coefficient of the NC-antenna shown in Fig. 7*b*, it is observed that the resonance frequency of the dipolar slot alone (with no FSS, on the other side of the substrate) happens at frequency lower than 57 GHz while the designed antenna shows two resonances above 57 GHz which is indeed the direct impact of forming the cavity by placing the FSS over the ground plane.

The radiation patterns of the fabricated antenna are measured and compared with the full-wave simulated ones in both *E* and *H* planes (*zy* and *zx* planes as shown in Fig. 5, respectively) at 58.5, 59.5 and 60.5 GHz, as shown in Fig. 8. Simulated and measured results are in good agreement. However, due to the fact that the feeding line and the probe-landing area are placed in the *E*-plane of the antenna, there are some differences and asymmetry between the *E*-plane measured and simulated radiation patterns. Fig. 9 shows the measured co-pol and cross-pol patterns of the antenna, in both *E* and *H* planes, at the resonance frequency of the antenna (i.e. 59.5 GHz). It can be seen that the cross-pol gain level of the antenna is 25 dB lower than its maximum gain at broadside.

The full-wave simulated radiation efficiency of the fabricated antenna (i.e. using a 12×12 element FSS printed on the substrate extended 1.5 mm on each side) shows a 95% efficiency at 59.5 GHz, including both conduction and dielectric losses.

4 Conclusion

An easy-to-fabricate, highly efficient planar single-feed single-layer 60 GHz FPC antenna, based on a simple design procedure, is proposed. The measurement results were compared with the simulated ones showing the feasibility of this design for 60 GHz wireless systems. The advantages and disadvantages of the proposed design are compared with the previous ones, designed at MMWs. The planar geometry of this antenna is very much desired for MMW applications and also for being integrated with other circuit elements on a single board (substrate) or even on-chip or in-package applications.

5 Acknowledgments

The authors acknowledge the support of ANSYS Corporation for the use of the simulation software (HFSS), Rogers Corporation for providing the substrate to fabricate the antenna (RT/duroid 5880) and the Broadcom Corporation, in particular Mr. Edward Roth, for providing some of the microwave components to build the test system.

6 References

1 Biglarbegian, B., Fakharzadeh, M., Nezhad-Ahmadi, M.R., Safavi-Naeini, S.: 'Optimized patch array antenna for 60 GHz wireless applications'. IEEE Int. Symp. Antennas Propagation, Toronto, ON, July 2010

2 Lovat, G., Burghignoli, P., Jackson, D.R.: 'Fundamental properties and optimization of broadside radiation from uniform leaky-wave antennas', *IEEE Trans. Antennas Propag.*, 2006, **54**, pp. 1442–1452

3 Zhao, T.X., Jackson, D.R., Williams, J.T., Oliner, A.A.: 'General formulas for 2-D leaky-wave antennas', *IEEE Trans. Antennas Propag.*, 2005, **53**, pp. 3525–3533

4 Ostner, H., Schmidhammer, E., Detlefsen, J., Jackson, D.R.: 'Radiation from dielectric leaky-wave antennas with circular and rectangular apertures', *Electromagnetics*, 1997, **17**, pp. 505–535

5 Sauleau, R., Coquet, P., Matsui, T.: 'Low-profile directive quasi-planar antennas based on millimeter wave Fabry–Perot cavities', *Proc. Microw. Antennas Propag.*, 2003, **150**, pp. 274–278

6 Lee, Y., Lu, X., Hao, Y., Yang, S., Evans, J.R.G., Parini, C.G.: 'Low-profile directive millimeter-wave antennas using free-formed three-dimensional (3-D) electromagnetic bandgap structures', *IEEE Trans. Antennas Propag.*, 2009, **57**, pp. 2893–2903

7 Hosseini, S.A., Capolino, F., De Flaviis, F.: 'Design of a single-feed all-metal 63 GHz Fabry–Perot cavity antenna using a TL and a wideband circuit model'. IEEE Int. Symp. Antennas Propagation, Charleston, SC, June 2009

8 Hosseini, S.A., Capolino, F., De Flaviis, F.: 'Single-feed highly-directive Fabry–Perot cavity antenna for 60 GHz wireless systems: design and fabrication'. IEEE Int. Symp. Antennas Propagation, Toronto, ON, July 2010

9 Hosseini, S.A., De Flaviis, F., Capolino, F.: 'A highly directive single-feed Fabry–Perot cavity antenna for 60 GHz technology'. IEEE Int. Symp. Antennas Propagation, Chicago, IL, July 2012

10 Gardelli, R., Albani, M., Capolino, F.: 'Array thinning by using antennas in a Fabry–Perot cavity for gain enhancement', *IEEE Trans. Antennas Propag.*, 2006, **54**, pp. 1979–1990

11 Felsen, L.B., Marcuvitz, N.: 'Radiation and scattering of waves' (Wiley, NY, 2003, 2nd edn.)

12 Chu, H., Guo, Y.-X., Wang, Z.: '60-GHz LTCC wideband vertical off-center dipole antenna and arrays', *IEEE Trans. Antennas Propag.*, 2013, **61**, (1), pp. 153–161

doi: 10.1049/iet-map.2014.0408